A Bacterial Artificial Chromosome Transgene with Polymorphic *Cd72* Inhibits the Development of Glomerulonephritis and Vasculitis in MRL-*Fas*^{lpr} Lupus Mice

Hisashi Oishi,*,†,[1] Takahito Tsubaki,†,[1] Tatsuhiko Miyazaki,† Masao Ono,‡ Masato Nose,†,‡,§ and Satoru Takahashi*

Systemic lupus erythematosus is considered to be under the control of polygenic inheritance, developing according to the cumulative effects of susceptibility genes with polymorphic alleles; however, the mechanisms underlying the roles of polygenes based on functional and pathological genomics remain uncharacterized. In this study, we substantiate that a CD72 polymorphism in the membrane-distal extracellular domain impacts on both the development of glomerulonephritis and vasculitis in a lupus model strain of mice, MRL/MpJ-*Fas*^{lpr}, and the reactivity of BCR signal stimulation. We generated mice carrying a bacterial artificial chromosome transgene originating from C57BL/6 (B6) mice that contains the *Cd72*^{b} locus (*Cd72*^{B6} transgenic [tg]) or the modified *Cd72*^{b} locus with an MRL-derived *Cd72*^{c} allele at the polymorphic region corresponding to the membrane-distal extracellular domain (*Cd72*$^{B6/MRL}$ tg). *Cd72*^{B6} tg mice, but not *Cd72*$^{B6/MRL}$ tg mice, showed a significant reduction in mortality following a marked improvement of disease associated with decreased serum levels of IgG3 and anti-dsDNA Abs. The number of splenic CD4^{-}CD8^{-} T cells in *Cd72*^{B6} tg mice was decreased significantly in association with a reduced response to B cell receptor signaling. These results indicate that the *Cd72* polymorphism affects susceptibility to lupus phenotypes and that novel functional rescue by a bacterial artificial chromosome transgenesis is an efficient approach with wide applications for conducting a genomic analysis of polygene diseases. ***The Journal of Immunology*****, 2013, 190: 2129–2137.**

Systemic lupus erythematosus (SLE) is a representative prototype of a systemic autoimmune disease in which the lethal hallmark is lupus nephritis and, occasionally, systemic vasculitis, associated with hypergammaglobulinemia and the production of Abs directed against a broad range of self-Ags (1). Etiologically, SLE is a disease of polygenic disorders that develop according to the cumulative effects of multiple genes with polymorphic alleles. A current and important issue is the detection of the genes that affect the complex pathological phenotypes of SLE and the clarification of their functional pathogenesis (2). However, little is known about the direct relationship between gene polymorphisms and the pathology of the disease.

MRL/MpJ-*Fas*^{lpr} (MRL-*Fas*^{lpr}) mice carrying a loss-of-function mutation in the *Fas* gene spontaneously develop systemic autoimmune diseases involving glomerulonephritis, vasculitis, arthritis, and sialadenitis associated with the production of autoantibodies and circulating immune complexes and show cytokine abnormalities similar to SLE (3, 4). Because MRL mice expressing the intact *Fas* gene show only mild disease with aging, it is known that the *Fas*^{lpr} mutation plays a crucial role in immunological abnormalities in these mice, probably by perturbing peripheral B cell tolerance (5–7). However, the development of disease phenotypes in MRL-*Fas*^{lpr} mice also requires the genetic background of an MRL strain of mice in addition to *Fas* mutations (8–10). By crossing MRL-*Fas*^{lpr} mice with a nonautoimmune disease–prone strain of mice, C3H/HeJ-*Fas*^{lpr} (C3H-*Fas*^{lpr}), we previously mapped *Agnm1* loci and *Arvm1* loci on chromosome 4 as the susceptibility loci to glomerulonephritis and vasculitis, respectively (11, 12). These loci are located in the same chromosomal region in which *Cd72* was identified as the most likely candidate gene because the extracellular domain of the CD72 molecule was polymorphic between MRL and C3H mice (12, 13). MRL mice, as well as NOD mice, express the *Cd72*^{c} allele, whereas C3H mice express the *Cd72*^{b} allele, as is the case for C57BL/6 (B6), NZB, and BXSB mice (13, 14). Compared with CD72^{a} and CD72^{b}, CD72^{c} contains a remarkable polymorphic region in the membrane-distal extracellular domain encoded by exon 8 that involves a 7-aa deletion caused by aberrant splicing at the intron 7/exon 8 junction and 13 aa substitutions. The sub-

*Department of Anatomy and Embryology, Graduate School of Comprehensive Human Sciences, University of Tsukuba, Tsukuba 305-8575, Japan; †Department of Pathogenomics, Ehime University Graduate School of Medicine, Ehime 791-0295, Japan; ‡Department of Histopathology, Tohoku University Graduate School of Medicine, Sendai 980-8575, Japan; and §Proteo-Medicine Research Center, Ehime University, Ehime 791-0295, Japan

[1]H.O. and T.T. contributed equally to this work.

Received for publication August 9, 2012. Accepted for publication December 21, 2012.

This work was supported by a Grant-in-Aid for Scientific Research and a grant of the Genome Network Project of the Ministry of Education, Culture, Sports, Science and Technology (to M.N. and S.T.) and a grant from the Research Funds of the Ministry of Health and Welfare of Japan (to M.N.).

Address correspondence and reprint requests to Prof. Masato Nose and Prof. Satoru Takahashi, Department of Histopathology, Tohoku University Graduate School of Medicine, Seiryo-machi 1-2, Aoba-ku, Sendai, Miyagi 980-8575, Japan (M.N.) and Department of Anatomy and Embryology, University of Tsukuba, Graduate School of Comprehensive Human Sciences, 1-1-1 Tennodai, Tsukuba 305-8575, Japan (S.T.). E-mail addresses: masanose@med.tohoku.ac.jp (M.N.) and satoruta@md.tsukuba.ac.jp (S.T.)

The online version of this article contains supplemental material.

Abbreviations used in this article: B6, C57BL/6; BAC, bacterial artificial chromosome; BUN, blood urea nitrogen; C3H-*Fas*^{lpr}, C3H/HeJ-*Fas*^{lpr}; FO, follicular zone; MRL-*Fas*^{lpr}, MRL/MpJ-*Fas*^{lpr}; MZ, marginal zone; SLE, systemic lupus erythematosus; tg, transgenic.

stitutions may cause considerable structural differences compared with the other alleles, which likely leads to functional alterations. CD72 negatively regulates BCR signaling by recruiting tyrosine phosphatase SHP-1 to its ITIM at the cytoplasmic region (15). The negative-regulatory role of CD72 causes CD72-deficient B cells to be hyperresponsive following BCR stimulation (16). However, it is still unclear whether the CD72 polymorphism is involved in the development of lupus-like diseases in MRL-*Fas*^{lpr} mice.

To identify the genes associated with complex disease traits, linkage analyses and subsequent congenic mapping were most effective (17). However, generating recombinant congenic strains of mice with particular phenotypes in conjunction with recombination at desired loci is challenging. In the current study, we performed complementation rescue of the autoimmune phenotypes in MRL-*Fas*^{lpr} mice using transgenesis of a bacterial artificial chromosome (BAC) carrying the *Cd72*^{b} allele without any additional enhancers. We generated two strains of BAC transgenic (tg) MRL-*Fas*^{lpr} mice: one carrying the *Cd72*^{b} locus originating from the genomic DNA of B6 mice (*Cd72*^{B6} tg mice) and another carrying the modified *Cd72*^{b} locus in which polymorphic exon 8 was replaced by MRL-derived exon 8 of the *CD72*^{c} allele (*Cd72*$^{B6/MRL}$ tg mice). We then examined lupus phenotypes in *Cd72*^{B6} tg and *Cd72*$^{B6/MRL}$ tg MRL-*Fas*^{lpr} mice. We demonstrate that transgenesis of *Cd72*^{B6} mice, but not *Cd72*$^{B6/MRL}$ mice, rescues MRL-*Fas*^{lpr} mice from autoimmune diseases, strongly suggesting that CD72^{c} plays a crucial role in the development of autoimmune diseases in these mice.

Materials and Methods

Generation of BAC tg mice

MRL-*Fas*^{lpr} mice were purchased from Charles River Laboratories (Shizuoka, Japan). The RP23-195K8 BAC clone (178,592 bp), which is constructed from the female B6 mouse, includes the upstream 110 kbp and downstream 60 kbp of the *Cd72* gene and was purchased from Invitrogen (Carlsbad, CA). For the modification of the membrane-distal extracellular domain of *Cd72*^{b} on the BAC DNA to the *Cd72*^{c} derived from an MRL mouse, we performed Pfu quick-change mutagenesis PCR (KOD plus; Toyobo, Japan) from genomic DNA of an MRL-*Fas*^{lpr} mouse kidney with the following primers: 5′-GAGAGATCTTA-GAGGAGTTGCTAGATCGTT-3′ flanked by a BglII site and 5′-GAGAGTCGACTGCTGGAGGAATAGCAGTCT-3′ flanked by a SalI site. The PCR product, which is 1531 bp in length and corresponds to the genomic sequence from exons 7 to 9 of the *Cd72* gene, was digested with BglII and SalI and ligated into a BamHI- and SalI-digested pKOV-KanF vector, as shown in Supplemental Fig. 1. The nucleotide positions from 62,121 to 63,649 bp of the RP23-195K8 BAC clone including intron 7 to exon 8 of the *Cd72*^{b} gene were exchanged to the PCR product which corresponds to the *Cd72*^{c} allele, according to Lalioti's protocol (18). The mutation resulted in the substitution of A to C at position 63,613 in the RP23-195K8 BAC DNA, which causes the acceptor site of exon 8 of the *Cd72* gene to shift backward and deletes 7 aa (RQDSDSQ) between aa 306–312 in the CD72 molecule. A circular, original BAC DNA (RP23-195K8) and a modified BAC DNA (RP23-195K8$^{g.62,121_63,649conMRL}$) were microinjected into the pronuclei of fertilized eggs from MRL-*Fas*^{lpr} mice, respectively. Tg mice were continuously bred with MRL-*Fas*^{lpr} mice and maintained with a complete MRL genetic background. All experiments were performed according to the *Guide for the Care and Use of Laboratory Animals* at the University of Tsukuba.

Quantitative real-time RT-PCR analysis

Total RNA was prepared from the MACS-sorted splenic CD19^{+} B cells of each tg line at 6–10 wk of age, and cDNA was synthesized. Real-time RT-PCR analysis was performed using Platinum SYBR Green qPCR SuperMix-UDG (Invitrogen), according to the manufacturer's protocol. Assays were performed in duplicate with the ABI PRISM 7700 system (Applied Biosystems). The oligonucleotide primers for transgene-derived *Cd72* were 5′-GGCAGCATTCGATGAACCTT-3′ (forward; *Cd72 ex6 Fw*) and 5′-CGATCTAGCAACTCCTCTAAGCC-3′ (reverse; *Cd72 ex7 Rv2*). The primers for endogenous *Cd72* were 5′-GGCAGCATTCAATGACCCTC-3′ (forward; *Cd72 ex6 Fw3*) and *Cd72 ex7 Rv2*. The primers for total *Cd72* were *Cd72 ex6 Fw*, *Cd72 ex6 Fw3*, and *Cd72 ex7 Rv2*. The primers for hypoxanthine phosphoribosyltransferase (*Hprt*) were 5′-CAAACTTTGC-TTTCCCTGGT-3′ (forward; *Hprt F*) and 5′-CAAGGGCATATCCAAC-AACA-3′ (reverse; *Hprt R*).

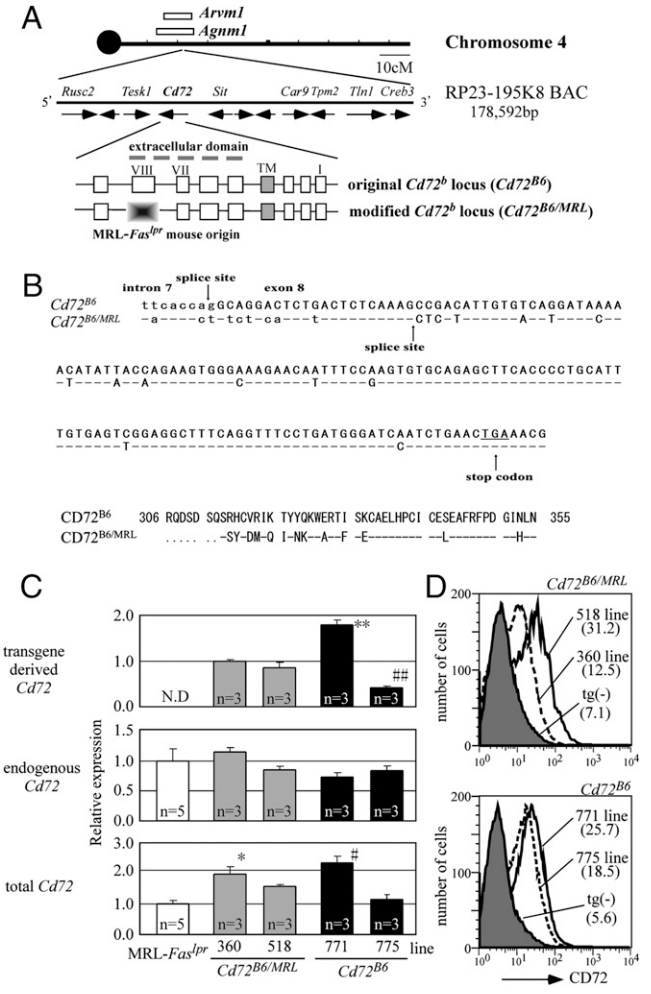

FIGURE 1. Generation of *Cd72*$^{B6/MRL}$ and *Cd72*^{B6} BAC tg mice. (**A**) Outline of BAC tg mouse lines with original RP23-195K8 BAC DNA (*Cd72*^{B6}) and modified RP23-195K8 BAC DNA (*Cd72*$^{B6/MRL}$). The modified RP23-195K8 BAC DNAs were generated by replacing the *Cd72* genomic sequence from intron 7 to exon 8 of the original BAC DNA with the homologous sequence derived from MRL-*Fas*^{lpr} mice. (**B**) DNA sequence of the original BAC (*Cd72*^{B6}) and the modified BAC (*Cd72*$^{B6/MRL}$) at the intron 7/exon 8 junction (*upper panel*). Deduced amino acid sequence of the region encoded by exon 8 from aa 306–355 on CD72^{B6} and CD72$^{B6/MRL}$ (*lower panel*). (**C**) Quantitative real-time RT-PCR analysis of *Cd72* mRNA. RNA was prepared from the MACS-sorted splenic CD19^{+} B cells of each tg line when the mice were 6–10 wk of age. The bar graphs show the average ± SEM. The expression levels in the 771 line are significantly higher than in mice of the other lines; the endogenous *Cd72* expression is downregulated, yielding a net *Cd72* expression level equal to that observed in the 360 line. (**D**) CD72 expression in splenic CD19^{+}-gated B cells in mice 6–8 wk of age. Numbers in parentheses are mean fluorescence index. Data are representative results obtained from three independent experiments. $^{**}p < 0.01$, versus the 360, 518, and 775 lines, $^{\#\#}p < 0.01$, versus the 360, 518, and 771 lines, $^{*}p < 0.05$, versus the MRL-*Fas*^{lpr} and 775 lines, $^{\#}p < 0.05$, versus the MRL-*Fas*^{lpr}, 518, and 775 lines. TM, Transmembrane domain.

Transgene copy number analysis of genomic DNA and transgene genotyping

The transgene copy number was determined by a real-time quantitative PCR method. The following primers in the RP23-195K8 BAC sequences were used for the transgene 5′-GAACACGCATTGGCCTACTC-3′ (for-

ward), 5′-TCATCGGGAAGGTAGCCAATC-3′ (reverse) and the reference gene (*mIL2*), 5′-CTAGGCCACAGAATTGAAAGATCT-3′ (forward), 5′-GTAGGTGGAAATTCTAGCATCATCC-3′ (reverse). The Platinum SYBR Green qPCR SuperMix UDG (Invitrogen) was used for the real-time amplification, according to the manufacturer's protocol. The assays were performed in duplicate on an ABI PRISM 7700 system (Applied Biosystems). Transgene-positive mice were identified by PCR using specific primers for the pBeloBAC11 vector. The oligonucleotide primers were 5′-AGTGTCACCTAAATAGCTTG-3′ (forward) and 5′-CAGTACTGCGATGAGTGGCA-3′ (reverse).

Histopathologic and immunohistologic examinations

Tissue samples were fixed with 10% formalin in 0.01 mol/l phosphate buffer (pH 7.2) and embedded in paraffin. They were stained with H&E for histological examination by light microscopy. The severity of the diseases was evaluated according to the previously proposed criteria for glomerulonephritis and renal vasculitis (10–12). In brief, glomerulonephritis was estimated as follows; grade 0 is normal, grade 1 has limited segmental mesangial proliferation, grade 2 has endocapillary proliferation with wire loop and/or hyaline thrombotic lesions, and grade 3 has dominant sclerosing and/or hyalinosis of the lesions in grade 2. The renal vascular lesions were graded as follows: grade 0 is normal-to-minimal perivascular lymphocytes infiltration, grade 1 is moderate perivascular cell infiltration associated with destruction of external elastic lamina, and grade 2 is the above findings plus intimal thickening with the destruction of internal elastic lamina. Frozen renal sections for the immunofluorescence analyses were stained with FITC-labeled anti-mouse IgG, IgM, IgG3, and C3 Abs (ICN Pharmaceuticals, Cleveland, OH). The average fluorescence intensity ≥20 glomeruli from each kidney section was quantified by analyzing the fluorescence microscopy images using ImageJ software (http://rsb.info.nih.gov/ij).

Serum levels of Igs, anti-dsDNA autoantibody titers, creatinine, and blood urea nitrogen

Total serum Ig was determined by the Mouse Ig ELISA Quantitation kits (Bethyl Laboratories, Montgomery, TX) and the TMB Microwell Peroxidase Substrate system (KPL, Gaithersburg, MD), according to the manufacturer's protocols. Anti-dsDNA autoantibody titers were measured by ELISA, as described previously (19). Arbitrary units were calculated using the linear ranges of the dilution and the standard curves generated with the pooled sera of old MRL-*Fas*^{lpr} mice. The concentration of serum creatinine and blood urea nitrogen (BUN) was measured by an automated analyzer (DRI-CHEM 3500) for routine laboratory tests at 20 wk of age (Fuji Film, Tokyo, Japan).

Abs and flow cytometry

We used the following mAbs for flow cytometric analysis: FITC-, PE-, PerCP-, or biotin-conjugated anti-CD3, anti-CD5, anti-B220, anti-CD21, anti-CD23, anti-Thy1.2, anti-CD4, anti-CD8, and anti-CD43. All Abs were from BD Pharmingen. For the expression analysis of CD72, an anti-CD72.4 Ab (CT-72.4; Cedarlane) was used. Cell surface staining was performed according to standard techniques, and the flow cytometric analysis was done with a FACSCalibur using CellQuest software (BD Biosciences, San Jose, CA).

Isolation of splenic B cells and viability assays

Splenic B cells from 6–8-wk-old mice were purified by negative selection using a MACS system with a B cell isolation kit (Miltenyi Biotec, Auburn, CA). The resulting splenic B cells (1×10^5 cells/ml) were stimulated by 15 μg/ml F(ab′)$_2$ goat anti-IgM Ab, 10 μg/ml anti-CD40 Ab, 15 μg/ml F(ab′)$_2$ goat anti-IgM Ab + 10 μg/ml anti-CD40, 10 μg/ml LPS, and 10 U/ml IL-4 (BD Biosciences) in flat-bottom 96-well microtiter plates for 3 d. After 68 h, the cells were pulsed with 20 μl/well of the vital dye CellTiter96 AQueous One Solution Reagent (Promega). B cell viability was determined by measurement of light absorbance at 490 nm, according to the manufacturer's manual.

Intracellular calcium response

Calcium mobilization of the splenic cells was measured using a BD LSR (Becton Dickinson). Erythrocyte-depleted splenocytes were loaded with 5 μM Fluo-4 AM ester (Dojindo, Kumamoto, Japan). Cells (1×10^7 cells) were stained with PE-conjugated CD19 Ab and stimulated with 20 μg/ml F(ab′)$_2$ goat anti-IgM Ab (Jackson ImmunoResearch Laboratories). The increases in intracellular calcium mobilization were presented as increased FL-1 fluorescence intensity following Ab treatment.

Kinetics of phosphorylation of ERK

Mouse lymphocytes from 6–8-wk-old mice were positively sorted for CD19$^+$ B cells using MACS CD19 microbeads. CD19$^+$ B cells (5×10^6 cells) were stimulated by adding 10 μg/ml F(ab′)$_2$ goat anti-IgM Ab. The cells were incubated for 0, 3, or 5 min at 37°C and were fixed by 2% formaldehyde, followed by 90% methanol. The cells were washed and loaded with Alexa Fluor 488–conjugated anti–phospho-p44/p42 MAPK Ab (E10; Cell Signaling Technology, Beverly, MA) and stained with a PE-conjugated anti-B220 Ab. The kinetics of p-ERK from the splenic cells were measured using a BD LSR.

Statistical analysis

Data are expressed as mean ± SEM. The comparison of two groups was performed using a one-way ANOVA, and a post hoc Bonferroni correction was used for multiple comparisons. The unpaired Student *t* test was used to compare two groups. The comparisons of survival rates were performed with the Kaplan–Meier method, with differences in the survival curves evaluated with a log-rank sum testing. A p value < 0.05 was considered statistically significant.

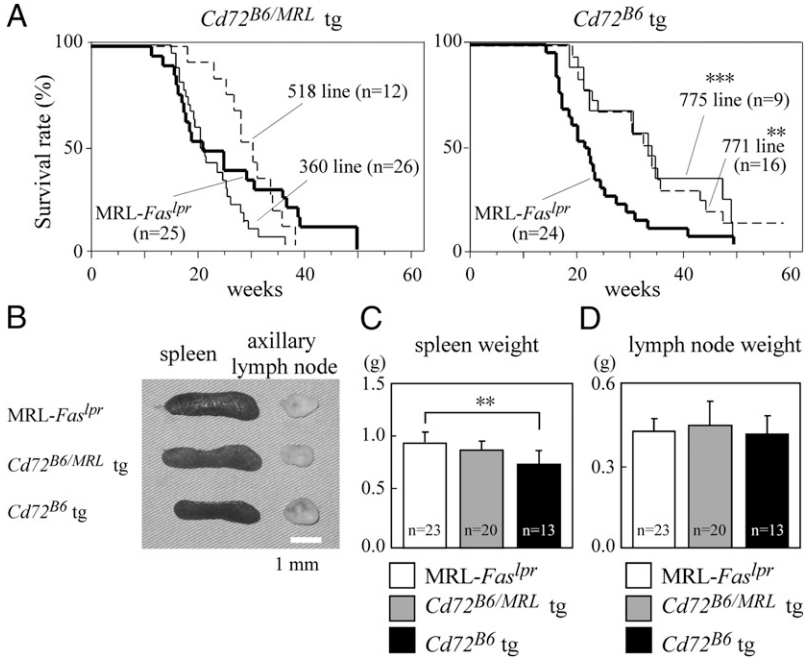

FIGURE 2. Extension of life span and reduced splenomegaly by *Cd72*^{B6} BAC transgenesis. (**A**) Kaplan–Meier analysis of survival of *Cd72*^{B6} and *Cd72*$^{B6/MRL}$ tg and MRL-*Fas*^{lpr} mice. *Left panel*, *Cd72*$^{B6/MRL}$ tg mice (lines 360 and 518). *Right panel*, *Cd72*^{B6} tg mice (lines 771 and 775). Data for MRL-*Fas*^{lpr} mice were obtained from the *Cd72* tg–negative littermate mice as control for both 360 and 518 lines (*left panel*) or for both 771 and 775 lines (*right panel*), respectively. (**B**) Gross appearance of the spleen and the axillary lymph node of MRL-*Fas*^{lpr}, *Cd72*$^{B6/MRL}$ tg, and *Cd72*^{B6} tg mice at 20 wk of age. (**C**) Mouse spleen weight at 20 wk of age. Bar graphs show average ± SEM. (**D**) Axillary lymph node weight at 20 wk of age. Bar graphs show average ± SEM. $^{**}p < 0.01$, $^{***}p < 0.001$.

Results

Generation and molecular characterization of $Cd72^{B6/MRL}$ *and* $Cd72^{B6}$ *BAC tg mice*

A *Cd72* polymorphism is accumulated in exon 8 encoding the C-terminal half of the C-type lectin-like domain in the extracellular region (Fig. 1A, 1B). Therefore, we replaced the region covering exon 8 in $Cd72^{b}$ in RP23-195K8 plasmid with that of $Cd72^{c}$ obtained from MRL mice using homologous recombination (Supplemental Fig. 1), which resulted in the BAC clone encoding a chimeric CD72 ($CD72^{b/c}$). This $CD72^{b/c}$ protein consists of the N-terminal region (amino acid positions 1–305) derived from $CD72^{B6}$ and the C-terminal region (amino acid positions 306–355) derived from $CD72^{MRL}$ where a 7-aa deletion and 13 aa substitutions exist (Fig. 1B). The original and modified BAC DNAs were microinjected into MRL-Fas^{lpr} fertilized oocytes to generate tg mice designated as $Cd72^{B6}$ tg, lines 771 and 775, and $Cd72^{B6/MRL}$ tg, lines 360 and 518 (Supplemental Fig. 2). Littermates negative for the transgene (non-BAC tg mice) were described as MRL-Fas^{lpr} mice. Quantitative PCR using genomic DNA revealed the copy numbers of the tg BACs in the 771, 775, 360, and 518 lines to be two, two, three, and five, respectively.

We first examined the expression of tg CD72 in splenic $CD19^{+}$ B cells. When mice of these lines were 6–10 wk old, quantitative RT-PCR analysis was performed with primers specific for the transgene-derived, endogenous, and total *Cd72* transcript (Fig. 1C, Supplemental Fig. 3). Transgene-derived *Cd72* was expressed in all tg lines, and its expression levels were almost compatible with those of endogenous *Cd72*. In the FACS analysis of splenic B cells, the expression level of a transgene-derived CD72 product identified in mice of every tg line and the expression levels in mice of lines 518 and 771 were relatively high (Fig. 1D). Endogenous $CD72^{MRL}$ ($CD72^{c}$) was not detected by the anti-CD72 Abs used in this analysis. These Abs may recognize an epitope on the polypeptides derived from $CD72^{B6}$ ($CD72^{b}$) at amino acid positions 1–305 but not at amino acid positions 306–354 (Fig. 1B). In addition, the expression levels of $CD72^{b}$ on spleen cells of B6 and $Cd72^{B6}$ tg mice were almost the same in FACS analysis (data not shown).

Reduced mortality and splenomegaly as a result of $Cd72^{B6}$ *BAC transgenesis*

Next, we analyzed the effects of $Cd72^{B6}$ and $Cd72^{B6/MRL}$ transgenes on survival in MRL-Fas^{lpr} mice using a Kaplan–Meier analysis (Fig. 2A). The life spans of both lines 771 and 775 $Cd72^{B6}$ tg mice were significantly longer than were those of MRL-Fas^{lpr} mice, whereas the life spans of both lines of $Cd72^{B6/MRL}$ tg mice were comparable to MRL-Fas^{lpr} mice. Further studies were performed

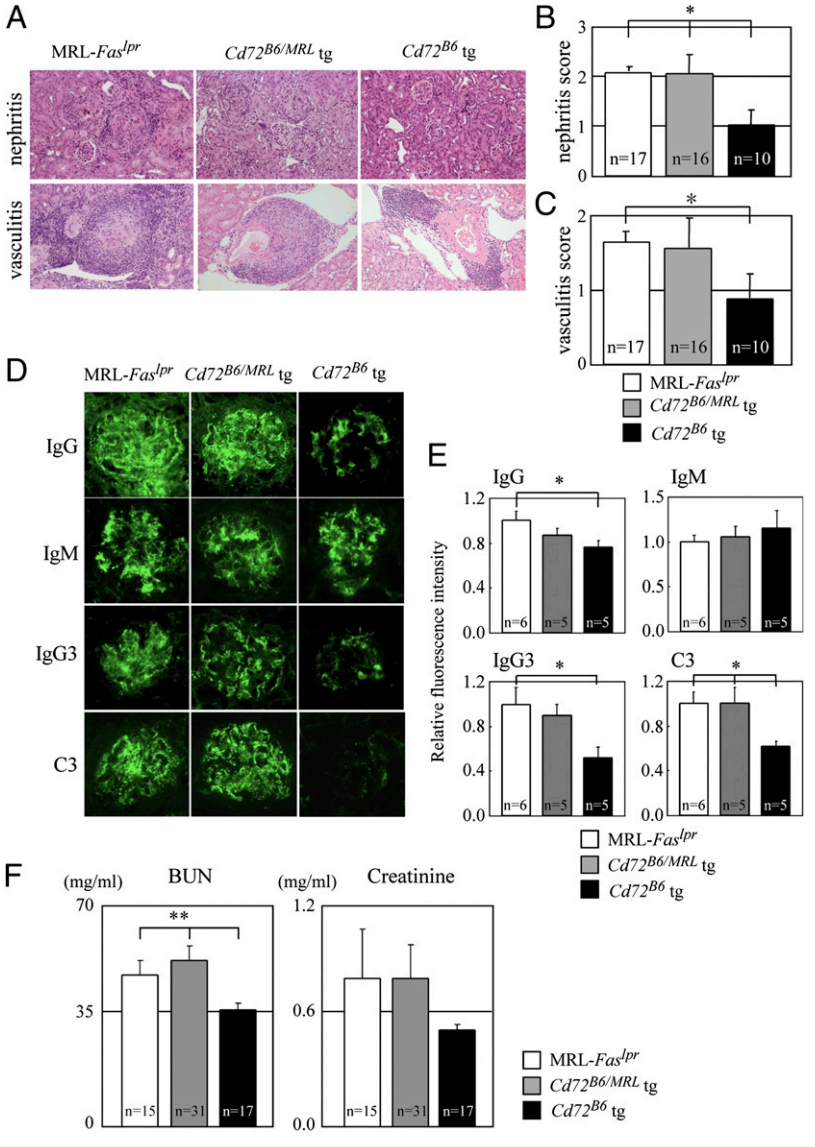

FIGURE 3. Decreased severities of glomerulonephritis and vasculitis in $Cd72^{B6}$ tg mice. (**A**) Representative histological manifestations of glomerulonephritis (*upper panels*) and renal vasculitis (*lower panel*) at 20 wk of age. H&E, original magnification ×100. (**B**) Semiquantitative analysis of the nephritis score. Data are average ± SEM. (**C**) Semiquantitative analysis of the vasculitis score. Data are average ± SEM. (**D**) Representative glomerular deposits of IgG, IgM, IgG3, and C3 in MRL-Fas^{lpr}, $Cd72^{B6/MRL}$ tg, and $Cd72^{B6}$ tg mice. IgG, IgG3, and C3 deposits were only suppressed in $Cd72^{B6}$ tg mice compared with MRL-Fas^{lpr} mice. Original magnification ×400. (**E**) Semiquantitative analysis of the immunofluorescence. Data are average ± SEM. (**F**) Serum BUN and serum creatinine levels in MRL-Fas^{lpr}, $Cd72^{B6/MRL}$ tg, and $Cd72^{B6}$ tg mice. Data are average ± SEM. $*p < 0.05$, $**p < 0.01$.

using *Cd72*$^{B6/MRL}$ tg, *Cd72*^{B6} tg, and MRL-*Fas*^{lpr} mice as a combination of lines 360 and 518, lines 771 and 775, and transgene-negative littermates, respectively.

Furthermore, the spleen weights of *Cd72*^{B6} tg mice, but not *Cd72*$^{B6/MRL}$ tg mice, at 20 wk of age were significantly reduced compared with those in MRL-*Fas*^{lpr} mice (Fig. 2B, 2C). Therefore, *Cd72*^{B6}, but not *Cd72*$^{B6/MRL}$, transgenesis reduces both mortality and splenomegaly in *MRL-Fas*^{lpr} mice. In contrast, no significant differences were observed in axillary lymph node weight at 20 wk of age among strains (Fig. 2D).

Cd72^{B6} *BAC transgenesis reduces the severity of glomerulonephritis and renal vasculitis*

Renal dysfunction is the major cause of death of MRL-*Fas*^{lpr} mice. A histopathological analysis of renal sections obtained at 20 wk of age revealed that the severity of both glomerulonephritis and vasculitis was markedly reduced in *Cd72*^{B6} tg mice, consistent with extended life spans (Fig. 3A). Scoring of the severity of both diseases revealed significant reductions in *Cd72*^{B6} tg mice compared with that observed in MRL-*Fas*^{lpr} mice, although the diseases were not completely inhibited (Fig. 3B, 3C). We then examined the deposits of IgG, IgM, IgG3, and C3 in the renal glomeruli using immunofluorescence staining (Fig. 3D). A semiquantitative analysis showed that IgG, IgG3 and C3 deposits, but not IgM deposits, were significantly decreased in *Cd72*^{B6} tg mice, but not in *Cd72*$^{B6/MRL}$ tg mice, compared with that observed in MRL-*Fas*^{lpr} mice (Fig. 3E). Furthermore, the serum BUN levels of *Cd72*^{B6} tg mice were significantly lower than those in MRL-*Fas*^{lpr} mice and *Cd72*$^{B6/MRL}$ tg mice at 20 wk of age (Fig. 3F). The serum creatinine levels of *Cd72*^{B6} tg mice were also lower than MRL-*Fas*^{lpr} and *Cd72*$^{B6/MRL}$ tg mice, although the differences were not statistically significant. Therefore, the expression of CD72^{B6}, but not CD72$^{B6/MRL}$, ameliorates glomerulonephritis with immune complex deposition in MRL-*Fas*^{lpr} mice. Interestingly, the presence of vascular lesions in *Cd72*^{B6} tg mice was limited only in perivascular mononuclear cell infiltration, whereas that in MRL-*Fas*^{lpr} and *Cd72*$^{B6/MRL}$ tg mice was associated with the destruction of the arterial external elastic laminae and media, thus indicating vasculitis (Fig. 3A, 3C). Although *Cd72*^{B6} BAC transgenesis ameliorated glomerulonephritis and vasculitis in MRL-*Fas*^{lpr} mice, other autoimmune manifestations, such as sialadenitis and arthritis, were not improved histopathologically (data not shown). This is consistent with the fact that quantitative trait loci for sialadenitis and arthritis of MRL-*Fas*^{lpr} mice were not mapped at a centromeric region of chromosome 4 in our previous studies using MRL-*Fas*^{lpr} × C3H-*Fas*^{lpr} crosses (20, 21).

Reduced expansion of lpr T cells and enhanced B cell maturation in Cd72^{B6} *tg spleens*

We next analyzed changes in the lymphocyte population in relation to any improvements in disease phenotypes in *Cd72*^{B6} tg mice. The total spleen cell number in *Cd72*^{B6} tg mice was significantly reduced compared with that in MRL-*Fas*^{lpr} and *Cd72*$^{B6/MRL}$ tg mice (Table I). Thymocyte cellularity and T cell development in *Cd72*^{B6} tg mice were comparable to that observed in MRL-*Fas*^{lpr} mice, as assessed by the percentages of CD4 and CD8 expression (Table I). However, in *Cd72*^{B6} tg mouse spleens, the numbers of T cells, especially those of CD4$^-$CD8$^-$ T cells, so-called "double-negative" *lpr* T cells, were reduced compared with those observed in MRL-*Fas*^{lpr} mouse spleens (*Cd72*^{B6} tg 74.0 ± 3.9%, $n = 5$; MRL-*Fas*^{lpr} 81.7 ± 0.9%, $n = 7$; *Cd72*$^{B6/MRL}$ tg 78.7 ± 4.1%, $n = 5$; $p < 0.05$) (Fig. 4B). Reductions in the expansion of *lpr* T cells appear to be involved in the improvement of macroscopic splenomegaly in *Cd72*^{B6} tg mice.

We next examined B cell components in *Cd72*^{B6} tg mice at 20 wk of age. In the bone marrow of *Cd72*^{B6} tg mice, the fre-

Table I. Cellular phenotypes in MRL-*Fas*^{lpr}, *Cd72*$^{B6/MRL}$ tg, and *Cd72*^{B6} tg mice

Population	MRL-*Fas*^{lpr} (n = 3–9)	*Cd72*$^{B6/MRL}$ tg (n = 3–5)	*Cd72*^{B6} tg (n = 3–6)
Bone marrow			
Total cell number (×10^6)	1.1 ± 0.17	0.8 ± 0.2	0.9 ± 0.1
Thymus			
Total cell number (×10^7)	3.9 ± 0.2	4.1 ± 0.9	3.9 ± 0.3
CD4$^+$CD8$^+$DP (×10^7)	1.2 ± 0.2	2.0 ± 0.2	1.5 ± 0.1
CD4$^+$SP (×10^7)	1.4 ± 0.1	1.2 ± 0.1	1.3 ± 0.1
CD8$^+$SP (×10^6)	7.1 ± 0.8	5.9 ± 0.4	7.0 ± 0.7
Spleen			
Total cell number (×10^8)	3.3 ± 0.7	3.8 ± 0.8	1.7 ± 0.4[a]
Thy1.2$^+$B220$^-$ (×10^8)	2.6 ± 0.5	2.9 ± 0.5	1.7 ± 0.5[a]
CD4$^+$SP (×10^7)	3.6 ± 0.6	4.2 ± 1.2	2.9 ± 0.6
CD8$^+$SP (×10^7)	1.0 ± 0.1	1.8 ± 0.5	0.8 ± 0.1
CD4$^-$CD8$^-$DN (×10^8)	2.4 ± 0.5	2.3 ± 0.4	0.9 ± 0.2[a]
B220$^+$CD3$^-$ (×10^7)	5.6 ± 2.0	4.5 ± 1.6	5.4 ± 1.1
T1 + T2 (×10^7)	1.6 ± 0.4	1.2 ± 0.3	1.4 ± 0.2
FO (×10^7)	1.7 ± 0.4	2.4 ± 0.5[b]	2.7 ± 0.6[a]
MZ (×10^7)	2.3 ± 0.9	5.8 ± 0.9[b]	7.1 ± 1.8[a]
Lymph nodes			
Total cell number (×10^8)	1.3 ± 0.1	0.8 ± 0.2	1.2 ± 0.5
Peritoneal cavity			
B-1a (×10^7)	1.4 ± 0.4	N.D.	0.9 ± 0.4[c]

Data for bone marrow and thymus were acquired when the mice were 8 wk of age; data for spleen, lymph nodes, and peritoneal cavity were acquired at ~20 wk of age.

Data are mean ± SEM.

[a] According to one-way ANOVA and post hoc Bonferroni correction, $p < 0.05$ versus MRL-*Fas*^{lpr} mice or *Cd72*$^{B6/MRL}$ tg mice.

[b] ANOVA and post hoc Bonferroni correction yielded statistically significant differences of $p < 0.05$ versus MRL-*Fas*^{lpr} mice.

[c] No statistically significant differences were found by unpaired Student t test.

B-1a, IgM$^+$CD5$^+$; DN, double negative; DP, double positive; FO, follicular zone B cell: B220$^+$CD3$^-$CD21^{low}CD23^{high}; MZ, marginal zone B cell: B220$^+$CD3$^-$CD21^{high}CD23$^{low/-}$; N.D., no data; SP, single positive; transitional 1 (T1) + transitional 2 (T2): B220$^+$CD3$^-$CD21$^{low/int}$CD23^{low}.

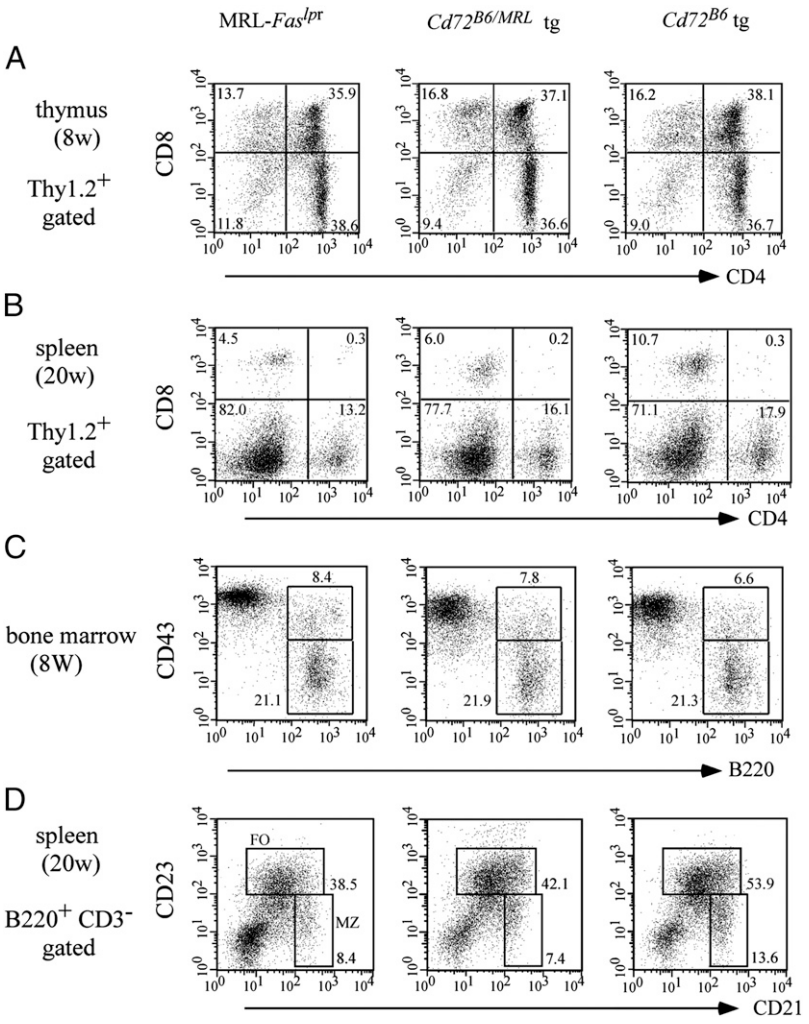

FIGURE 4. Enhanced B cell development and reduced *lpr* T cells in the spleen of *Cd72*^{B6} tg mice. Thy1.2$^+$-gated T cell populations in the thymus (**A**) and spleen (**B**). (**C**) B cell development in bone marrow. (**D**) B220$^+$CD3$^-$–gated B cell development in the spleen. FO, CD21^{low}CD23^{high}; MZ, CD21^{high}CD23$^{low/-}$.

quency of the pro-B cell subset (B220$^+$CD43$^+$) was decreased slightly compared with that observed in MRL-*Fas*^{lpr} mice; however, the frequency of the more differentiated B cell subset (B220$^+$CD43$^-$) was not different among the three genotypes (Fig. 4C). In spleens, the number of B220$^+$CD3$^-$ cells did not differ between MRL-*Fas*^{lpr} and *Cd72*^{B6} tg mice (Table I). However, the percentage of follicular zone (FO) B cells (CD21^{low} CD23^{high}) was increased in *Cd72*^{B6} tg mice compared with that observed in MRL-*Fas*^{lpr} mice (*Cd72*^{B6} tg 58.3 $\pm$ 8.1%, $n = 4$; MRL-*Fas*^{lpr} 36.3 $\pm$ 7.6%, $n = 7$; *Cd72*$^{B6/MRL}$ 42.7 $\pm$ 17.2%, $n = 4$; $p < 0.05$) (Fig. 4D). The percentage of marginal zone (MZ) B cells (CD21^{high}CD23$^{low/-}$) was increased slightly in *Cd72*^{B6} tg mice (*Cd72*^{B6} tg 12.6 $\pm$ 3.3%, $n = 4$; MRL-*Fas*^{lpr} 7.6 $\pm$ 3.6%, $n = 6$; *Cd72*$^{B6/MRL}$ tg 9.8 $\pm$ 4.9%, $n = 4$; NS) (Fig. 4D). Accordingly, the absolute numbers of FO and MZ B cells were significantly increased in *Cd72*^{B6} tg mice compared with those in MRL-*Fas*^{lpr} mice (Table I). The frequency of peritoneal B-1a cells was not different between *Cd72*^{B6} tg mice and MRL-*Fas*^{lpr} mice (Table I). In humans, it is reported that CD72 suppresses naive B cell differentiation to plasma cells by downregulating *XBP-1* (22). However, in our study, the percentage of CD138$^+$ cells in the mouse spleens and the *Xbp1* expression levels in splenic CD19$^+$ B cells showed no differences among the genotyped groups of mice (Supplemental Fig. 4). These results indicate that *Cd72*^{B6} transgenesis improves splenomegaly by reducing the number of *lpr* T cells and augmenting B cell maturation to FO and MZ B cells in the periphery while not affecting B cell differentiation to plasma cells.

Reduction of serum levels of IgG3 and anti-dsDNA Abs in Cd72^{B6} *tg mice*

The serum levels of Igs and autoantibodies were measured (Fig. 5). The IgG3 levels and anti-dsDNA autoantibody titers decreased significantly in *Cd72*^{B6} tg mice but not in *Cd72*$^{B6/MRL}$ tg mice. These results are consistent with our previous finding that the production of IgG3 in MRL-*Fas*^{lpr} mice is a major factor responsible for the development of glomerulonephritis (19).

Reduced survival and BCR signaling responses in B cells obtained from Cd72^{B6} *tg mice*

To examine proliferation of *Cd72*^{B6} and *Cd72*$^{B6/MRL}$ tg B cells in response to various mitogenic stimuli, we purified splenic B cells using negative selection with magnetic beads and stimulated the cells with anti-IgM F(ab′)$_2$ Abs in the presence or absence of anti-CD40 Abs or with LPS. Cell viability responding to these stimuli was significantly reduced in *Cd72*^{B6} tg, but not *Cd72*$^{B6/MRL}$ tg, B cells compared with that observed in MRL-*Fas*^{lpr} B cells (Fig. 6A).

To examine BCR signaling, we compared BCR-induced intracellular Ca^{2+} increases and kinetics of MAPK activation among the three groups of mice, because B cells from MRL-*Fas*^{lpr} mice show hyperactivity to BCR stimulation compared with that observed in other nonautoimmune mice (23). B cells from *Cd72*^{B6} tg mice showed decreased and shortened influxes of Ca^{2+} after stimulation with anti-IgM F(ab′)$_2$ Abs compared with those observed in B cells from MRL-*Fas*^{lpr} mice (Fig. 6B), whereas the Ca^{2+} response in *Cd72*$^{B6/MRL}$ tg B cells was similar to that in MRL-*Fas*^{lpr} B cells. Furthermore, the levels of phospho-p44/42

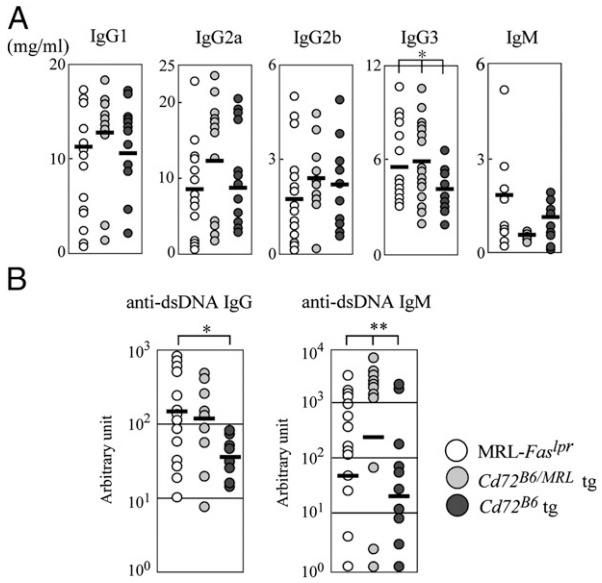

FIGURE 5. Decreased serum IgG3 levels and anti-dsDNA Ab titers in $Cd72^{B6}$ tg mice. (**A**) Serum Ig levels of each tg line. Serum IgG3 levels of $Cd72^{B6}$ tg mice at 20–24 wk of age were significantly reduced compared with MRL-Fas^{lpr} mice. The horizontal lines represent the average. (**B**) Serum titers of IgG and IgM anti-dsDNA. The horizontal lines represent the average. $*p < 0.05$, $**p < 0.01$.

MAPK, one of the major downstream pathways of BCR, were decreased in $Cd72^{B6}$ tg, but not in $Cd72^{B6/MRL}$ tg, B cells compared with MRL-Fas^{lpr} B cells (Fig. 6C). These results indicate that $Cd72^{B6}$, but not $Cd72^{B6/MRL}$, BAC transgenesis downregulates B cell responses to BCR ligation and other stimuli.

Discussion

To examine the impact of polymorphic *Cd72* as a positional candidate gene for autoimmune diseases in MRL-Fas^{lpr} mice, we generated transgenic MRL-Fas^{lpr} mice carrying a $Cd72^{b}$ locus by means of BAC, which is usually >100 kbp in length and reproduces a spatio-temporal expression pattern similar to that of the endogenous locus independently of its integration site (24). The BAC clone used in this study includes the upstream 110 kbp and downstream 60 kbp of the *Cd72* gene, suggesting that the expression of BAC-derived *Cd72* could be induced and distributed in tissues and stages of development in the tg mice in the same manner as endogenous *Cd72* under the control of the *cis*- and *trans*-elements. To adjust the expression levels of *Cd72*, as well as other involved genes on the BAC transgene, we compared tg MRL-Fas^{lpr} mice carrying a nonmodified and modified $Cd72^{b}$ locus in BAC DNA, both of which were identical in the DNA sequence, with the exception of the introduced mutation at the polymorphic sites of interest. Moreover, pronuclear injection of transgene into fertilized oocytes of MRL-Fas^{lpr} mice was performed to maintain a complete host genetic background, thereby preventing any issues related to genetic background. Although there might be a concern about the effect of integration sites of BAC on function, especially when multiple copies have integrated, a genomic-integration site of the transgene is typically confined to a single genomic site, regardless of the copy numbers (25). Furthermore, we revealed two independent tg lines of each group to avoid the risk that a DNA-integration site might reflect on different phenotypes in each group, which showed similar autoimmunity and mortality. Therefore, the results strongly suggest that phenotypic differences between $Cd72^{B6/MRL}$ mice and $Cd72^{B6}$ mice are dependent on the mutations within the BAC and not on the transgene copy numbers and their integration sites. Thus, this method enabled us to directly identify the role of the *Cd72* polymorphism in the development of autoimmune diseases in MRL-Fas^{lpr} mice.

CD72 is a negative regulator of BCR signaling (15, 26). The strength of the BCR signal is regulated by both positive and negative regulators for B cell homeostasis (27). In this study, we demonstrated that the $Cd72^{c}$ allele was a hypofunctional polymorphism of B cell signaling compared with the $Cd72^{b}$ allele; the B cells of $Cd72^{B6}$ tg mice showed a lower BCR signal strength than did $Cd72^{B6/MRL}$ tg mice, as demonstrated by the decrease in cell survival upon various stimuli, intracellular Ca^{2+} influx, and MAPK activation. This was remarkable, even subtracting for the possibility of the effects of endogenous $CD72^{c}$ of MRL-Fas^{lpr} mice and/or the dominant negative effects of the heterodimeric CD72 composed of $CD72^{c}$ and $CD72^{b}$. These effects may result in improved autoantibody production and lupus phenotypes in conjunction with reductions in mortality. The ligand binding sites of CD72 have not been mapped; however, the membrane-distal extracellular domain is considered to have an important role in ligand binding (28, 29). Therefore, the emphasized protective effects of BCR signaling in $Cd72^{B6}$ tg mice might depend on the receptor's affinity for its ligand.

The serum IgG3 levels in $Cd72^{B6}$ tg mice were significantly reduced compared with those in MRL-Fas^{lpr} and $Cd72^{B6/MRL}$ tg mice, although other IgG isotype expression levels were comparable among the three groups of mice. Production of IgG3 in MRL-Fas^{lpr} mice was shown to be a major factor responsible for the development of glomerulonephritis (19). The IgG3 expression levels in $Cd72^{-/-}$ mice were similar to those in wild-type mice, whereas $Cd72^{-/-}$ mice showed significantly lower levels of serum IgG3 to the T cell–dependent secondary responses (16). In contrast to IgM- and IgD-specific negative regulation by CD22, Ig class–specific regulation by CD72 was not detected in vivo (30). However, it may be possible that CD72 has unknown effects on the regulation of IgG3 specific in the MRL genetic background.

Several anti-DNA Abs have been produced by MZ B cells in other murine models of lupus including NZB/W F1 mice (31, 32). The autoimmunity of MRL-Fas^{lpr} mice was also reported to be involved in MZ B cells or B-1 cells as shown by the enlarged splenic MZ compartment and anti-Sm Ab transgenic study (33, 34). In addition, $Cd72^{-/-}$ mice showed an accumulation of pre-B cells in bone marrow and a reduction in the number of mature B cells in the periphery in combination with a slightly higher percentage of MZ B cells and increased numbers of B-1 cells (16). Whereas, in the current study, the proportion of MZ B cells and B-1 cells in $Cd72^{B6}$ tg mice were not decreased compared with MRL-Fas^{lpr} mice. Therefore, the disease improvement in $Cd72^{B6}$ tg mice seems to be independent of MZ B cells and B-1 cells. Indeed, a recent study indicates that MRL-Fas^{lpr} mice with a mutant B cell activating factor receptor showed decreased FO or MZ B cell subsets; however, this did not contribute to glomerulonephritis (35). Taken together, the pathological B cell population in MRL-Fas^{lpr} mice is different from that in NZB/W F1 mice.

Other quantitative trait loci associated with autoimmune disorders, such as *Lbw2* and *Sle2*, were mapped on chromosome 4, which were derived from other lupus-prone mice, NZB/W F1 and NZB2410, respectively (36, 37). However, NZB and NZW mice have the same $Cd72^{b}$ allele, suggesting that CD72 is not a common susceptibility gene in lupus-like phenotypes in NZB/W F1 and other related mice. In MRL-Fas^{lpr} mice, the polymorphisms of *Cd22*, *Fcgr2b*, *Spp1*, *IL10ra*, and *Coro1a* were reported to be associated with autoimmune phenotypes (11, 38–41). Of particular interest, the epistatic interaction between *Cd72* and *Fcgr2b* in the

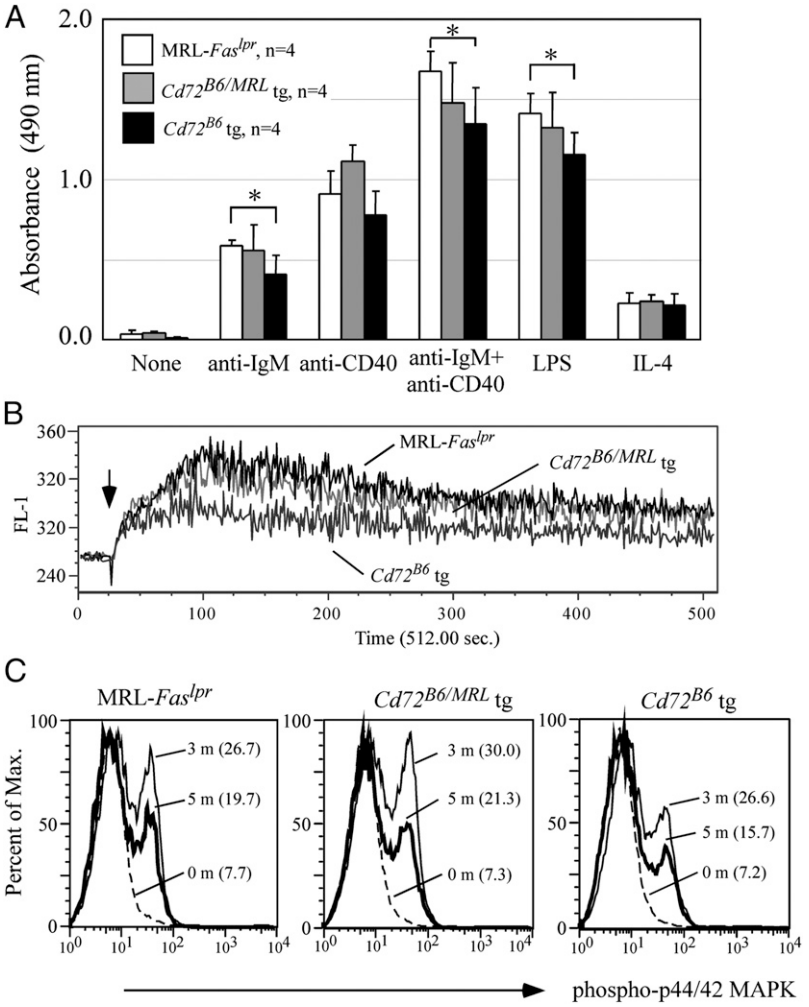

FIGURE 6. Hypoproliferation, decreased kinetics of intracellular Ca^{2+} response, and decreased MAPK activation of splenic B cells from *Cd72*^{B6} tg mice. (**A**) Survival of MACS-sorted splenic B cells from MRL-*Fas*^{lpr}, *Cd72*$^{B6/MRL}$, and *Cd72*^{B6} tg mice at 20 wk of age in response to various stimuli. All assays were performed in triplicate, and data are average ± SEM. A total of 15 μg/ml F(ab′)$_2$ goat anti-IgM Ab, 10 μg/ml anti-CD40 Ab, 15 μg/ml F(ab′)$_2$ goat anti-IgM Ab + 10 μg/ml anti CD40, 10 μg/ml LPS, and 10 U/ml IL 4 were used. (**B**) Intracellular Ca^{2+} response of splenic cells from MRL-*Fas*^{lpr}, *Cd72*$^{B6/MRL}$ tg, and *Cd72*^{B6} tg mice, following IgM cross-linking. Splenocytes were stimulated with 20 μg/ml of F(ab′)$_2$ goat anti-IgM Ab and then examined by flow cytometry for FL-1. Data are representative of three independent experiments that had similar results. The time of addition of stimuli is indicated by the arrow. (**C**) Flow cytometric analysis of B cells from MRL-*Fas*^{lpr}, *Cd72*$^{B6/MRL}$, and *Cd72*^{B6} tg mice, using a p-ERK Ab after the BCR stimulation [10 μg/ml F(ab′)$_2$ goat anti-IgM Ab] for 0, 3, or 5 min at 37°C. The values in parentheses are mean fluorescence index. Data are representative of four independent experiments with similar results. *$p < 0.05$.

development of autoimmune diseases has been observed in both humans and mice (42, 43). The occurrence of polygenic diseases has been explained in a threshold-liability model, in which individuals develop the disease when the total number of disease-susceptibility genes exceeds a given threshold. Therefore, it will be valuable to analyze the interactions of *Cd72* with other susceptible genes to elucidate the mechanisms of polygenic inheritance.

In this study, we demonstrated that a CD72 polymorphism in the membrane-distal extracellular domain is associated with glomerulonephritis and vasculitis in an autoimmune-prone mouse, owing to the hypofunctional allele of *Cd72*^{c}. These results suggest that CD72 is a target molecule for the therapeutic management of these diseases.

Acknowledgments

We thank Dr. Takeshi Tsubata for review of and advice on the manuscript; Dr. Maria D. Lalioti for providing vectors and helpful advice necessary to modify the BAC clone; and Miho Terada, Yuko Suzuki, Makiko Itakura, and Yukiyo Ida for technical assistance.

Disclosures

The authors have no financial conflicts of interest.

References

1. Rothfield, N. J. 1985. Systemic lupus erythematosus: clinical aspects and treatment. In *Arthritis and Allied Conditions.* D. J. McCarty, ed. Lea and Febiger, Philadelphia, p. 911–935.
2. Glazier, A. M., J. H. Nadeau, and T. J. Aitman. 2002. Finding genes that underlie complex traits. *Science* 298: 2345–2349.
3. Murphy, E. D., and J. B. Roths. 1978. Autoimmunity and lymphoproliferation: Induction by mutant gene lpr, and acceleration by a male-associated factor in strain BXSB mice. In *Genetic Control of Autoimmune Disease.* N. R. Rose, P. E. Bigazzi, and N. L. Warner, eds. Elsevier, New York, p. 207–220.
4. Andrews, B. S., R. A. Eisenberg, A. N. Theofilopoulos, S. Izui, C. B. Wilson, P. J. McConahey, E. D. Murphy, J. B. Roths, and F. J. Dixon. 1978. Spontaneous murine lupus-like syndromes. Clinical and immunopathological manifestations in several strains. *J. Exp. Med.* 148: 1198–1215.
5. Watanabe-Fukunaga, R., C. I. Brannan, N. G. Copeland, N. A. Jenkins, and S. Nagata. 1992. Lymphoproliferation disorder in mice explained by defects in Fas antigen that mediates apoptosis. *Nature* 356: 314–317.
6. Rathmell, J. C., M. P. Cooke, W. Y. Ho, J. Grein, S. E. Townsend, M. M. Davis, and C. C. Goodnow. 1995. CD95 (Fas)-dependent elimination of self-reactive B cells upon interaction with CD4+ T cells. *Nature* 376: 181–184.
7. Hao, Z., G. S. Duncan, J. Seagal, Y. W. Su, C. Hong, J. Haight, N. J. Chen, A. Elia, A. Wakeham, W. Y. Li, et al. 2008. Fas receptor expression in germinal-center B cells is essential for T and B lymphocyte homeostasis. *Immunity* 29: 615–627.
8. Theofilopoulos, A. N., and F. J. Dixon. 1985. Murine models of systemic lupus erythematosus. *Adv. Immunol.* 37: 269–390.
9. Nose, M., M. Nishimura, and M. Kyogoku. 1989. Analysis of granulomatous arteritis in MRL/Mp autoimmune disease mice bearing lymphoproliferative genes. The use of mouse genetics to dissociate the development of arteritis and glomerulonephritis. *Am. J. Pathol.* 135: 271–280.
10. Watson, M. L., J. K. Rao, G. S. Gilkeson, P. Ruiz, E. M. Eicher, D. S. Pisetsky, A. Matsuzawa, J. M. Rochelle, and M. F. Seldin. 1992. Genetic analysis of MRL-lpr mice: relationship of the Fas apoptosis gene to disease manifestations and renal disease-modifying loci. *J. Exp. Med.* 176: 1645–1656.
11. Miyazaki, T., M. Ono, W. M. Qu, M. C. Zhang, S. Mori, S. Nakatsuru, Y. Nakamura, T. Sawasaki, Y. Endo, and M. Nose. 2005. Implication of allelic polymorphism of osteopontin in the development of lupus nephritis in MRL/lpr mice. *Eur. J. Immunol.* 35: 1510–1520.
12. Qu, W. M., T. Miyazaki, M. Terada, L. M. Lu, M. Nishihara, A. Yamada, S. Mori, Y. Nakamura, H. Ogasawara, C. Yazawa, et al. 2000. Genetic dissection

of vasculitis in MRL/lpr lupus mice: a novel susceptibility locus involving the CD72c allele. *Eur. J. Immunol.* 30: 2027–2037.
13. Ying, H., E. Nakayama, W. H. Robinson, and J. R. Parnes. 1995. Structure of the mouse CD72 (Lyb-2) gene and its alternatively spliced transcripts. *J. Immunol.* 154: 2743–2752.
14. Rojas, A., F. Xu, M. Rojas, and J. W. Thomas. 2003. Structure and function of CD72 in the non-obese diabetic (NOD) mouse. *Autoimmunity* 36: 233–239.
15. Adachi, T., H. Flaswinkel, H. Yakura, M. Reth, and T. Tsubata. 1998. The B cell surface protein CD72 recruits the tyrosine phosphatase SHP-1 upon tyrosine phosphorylation. *J. Immunol.* 160: 4662–4665.
16. Pan, C., N. Baumgarth, and J. R. Parnes. 1999. CD72-deficient mice reveal nonredundant roles of CD72 in B cell development and activation. *Immunity* 11: 495–506.
17. Rogner, U. C., and P. Avner. 2003. Congenic mice: cutting tools for complex immune disorders. *Nat. Rev. Immunol.* 3: 243–252.
18. Lalioti, M., and J. Heath. 2001. A new method for generating point mutations in bacterial artificial chromosomes by homologous recombination in Escherichia coli. *Nucleic Acids Res*. 29:E14.
19. Takahashi, S., M. Nose, J. Sasaki, T. Yamamoto, and M. Kyogoku. 1991. IgG3 production in MRL/lpr mice is responsible for development of lupus nephritis. *J. Immunol.* 147: 515–519.
20. Nishihara, M., M. Terada, J. Kamogawa, Y. Ohashi, S. Mori, S. Nakatsuru, Y. Nakamura, and M. Nose. 1999. Genetic basis of autoimmune sialadenitis in MRL/lpr lupus-prone mice: additive and hierarchical properties of polygenic inheritance. *Arthritis Rheum.* 42: 2616–2623.
21. Kamogawa, J., M. Terada, S. Mizuki, M. Nishihara, H. Yamamoto, S. Mori, Y. Abe, K. Morimoto, S. Nakatsuru, Y. Nakamura, and M. Nose. 2002. Arthritis in MRL/lpr mice is under the control of multiple gene loci with an allelic combination derived from the original inbred strains. *Arthritis Rheum.* 46: 1067–1074.
22. Yamazaki, T., H. Nagumo, T. Hayashi, K. Sugane, and K. Agematsu. 2005. CD72-mediated suppression of human naive B cell differentiation by down-regulating X-box binding protein 1. *Eur. J. Immunol.* 35: 2325–2334.
23. Nijnik, A., H. Ferry, G. Lewis, E. Rapsomaniki, J. C. Leung, A. Daser, T. Lambe, C. C. Goodnow, and R. J. Cornall. 2006. Spontaneous B cell hyperactivity in autoimmune-prone MRL mice. *Int. Immunol.* 18: 1127–1137.
24. Van Keuren, M. L., G. B. Gavrilina, W. E. Filipiak, M. G. Zeidler, and T. L. Saunders. 2009. Generating transgenic mice from bacterial artificial chromosomes: transgenesis efficiency, integration and expression outcomes. *Transgenic Res.* 18: 769–785.
25. Lo, C. W., M. Coulling, and C. Kirby. 1987. Tracking of mouse cell lineage using microinjected DNA sequences: analyses using genomic Southern blotting and tissue-section in situ hybridizations. *Differentiation* 35: 37–44.
26. Hokazono, Y., T. Adachi, M. Wabl, N. Tada, T. Amagasa, and T. Tsubata. 2003. Inhibitory coreceptors activated by antigens but not by anti-Ig heavy chain antibodies install requirement of costimulation through CD40 for survival and proliferation of B cells. *J. Immunol.* 171: 1835–1843.
27. Grimaldi, C. M., R. Hicks, and B. Diamond. 2005. B cell selection and susceptibility to autoimmunity. *J. Immunol.* 174: 1775–1781.
28. Robinson, W. H., H. Ying, M. C. Miceli, and J. R. Parnes. 1992. Extensive polymorphism in the extracellular domain of the mouse B cell differentiation antigen Lyb-2/CD72. *J. Immunol.* 149: 880–886.
29. Kumanogoh, A., T. Shikina, C. Watanabe, N. Takegahara, K. Suzuki, M. Yamamoto, H. Takamatsu, D. V. Prasad, M. Mizui, T. Toyofuku, et al. 2005. Requirement for CD100-CD72 interactions in fine-tuning of B-cell antigen receptor signaling and homeostatic maintenance of the B-cell compartment. *Int. Immunol.* 17: 1277–1282.
30. Wakabayashi, C., T. Adachi, J. Wienands, and T. Tsubata. 2002. A distinct signaling pathway used by the IgG-containing B cell antigen receptor. *Science* 298: 2392–2395.
31. Grimaldi, C. M., D. J. Michael, and B. Diamond. 2001. Cutting edge: expansion and activation of a population of autoreactive marginal zone B cells in a model of estrogen-induced lupus. *J. Immunol.* 167: 1886–1890.
32. Zeng, D., M. K. Lee, J. Tung, A. Brendolan, and S. Strober. 2000. Cutting edge: a role for CD1 in the pathogenesis of lupus in NZB/NZW mice. *J. Immunol.* 164: 5000–5004.
33. Mandik-Nayak, L., S. J. Seo, C. Sokol, K. M. Potts, A. Bui, and J. Erikson. 1999. MRL-lpr/lpr mice exhibit a defect in maintaining developmental arrest and follicular exclusion of anti-double-stranded DNA B cells. *J. Exp. Med.* 189: 1799–1814.
34. Santulli-Marotto, S., Y. Qian, S. Ferguson, and S. H. Clarke. 2001. Anti-Sm B cell differentiation in Ig transgenic MRL/Mp-lpr/lpr mice: altered differentiation and an accelerated response. *J. Immunol.* 166: 5292–5299.
35. Ju, Z. L., G. Y. Shi, J. X. Zuo, and J. W. Zhang; Jian Sun. 2007. Unexpected development of autoimmunity in BAFF-R-mutant MRL-lpr mice. *Immunology* 120: 281–289.
36. Kono, D. H., R. W. Burlingame, D. G. Owens, A. Kuramochi, R. S. Balderas, D. Balomenos, and A. N. Theofilopoulos. 1994. Lupus susceptibility loci in New Zealand mice. *Proc. Natl. Acad. Sci. USA* 91: 10168–10172.
37. Morel, L., U. H. Rudofsky, J. A. Longmate, J. Schiffenbauer, and E. K. Wakeland. 1994. Polygenic control of susceptibility to murine systemic lupus erythematosus. *Immunity* 1: 219–229.
38. Lajaunias, F., N. Ibnou-Zekri, L. Fossati Jimack, Y. Chicheportiche, R. M. Parkhouse, C. Mary, L. Reininger, G. Brighouse, and S. Izui. 1999. Polymorphisms in the Cd22 gene of inbred mouse strains. *Immunogenetics* 49: 991–995.
39. Xiu, Y., K. Nakamura, M. Abe, N. Li, X. S. Wen, Y. Jiang, D. Zhang, H. Tsurui, S. Matsuoka, Y. Hamano, et al. 2002. Transcriptional regulation of Fcgr2b gene by polymorphic promoter region and its contribution to humoral immune responses. *J. Immunol.* 169: 4340–4346.
40. Qi, Z. M., J. Wang, Z. R. Sun, F. M. Ma, Q. R. Zhang, S. Hirose, and Y. Jiang. 2005. Polymorphism of the mouse gene for the interleukin 10 receptor alpha chain (Il10ra) and its association with the autoimmune phenotype. *Immunogenetics* 57: 697–702.
41. Haraldsson, M. K., C. A. Louis-Dit-Sully, B. R. Lawson, G. Sternik, M. L. Santiago-Raber, N. R. Gascoigne, A. N. Theofilopoulos, and D. H. Kono. 2008. The lupus-related Lmb3 locus contains a disease-suppressing Coronin-1A gene mutation. *Immunity* 28: 40–51.
42. Hitomi, Y., N. Tsuchiya, A. Kawasaki, J. Ohashi, T. Suzuki, C. Kyogoku, T. Fukazawa, S. Bejrachandra, U. Siriboonrit, D. Chandanayingyong, et al. 2004. CD72 polymorphisms associated with alternative splicing modify susceptibility to human systemic lupus erythematosus through epistatic interaction with FCGR2B. *Hum. Mol. Genet.* 13: 2907–2917.
43. Zhang, M. C., N. Misu, H. Furukawa, Y. Watanabe, M. Terada, H. Komori, T. Miyazaki, M. Nose, and M. Ono. 2006. An epistatic effect of the female specific loci on the development of autoimmune vasculitis and antinuclear autoantibody in murine lupus. *Ann. Rheum. Dis.* 65: 495–500.